DOI: 10.12737/stp-111202508

Received October 10, 2024 Accepted December 11, 2024

ANALYSIS OF THE EFFECT OF COSMIC NOISE ABSORPTION INCREASE ON PROPAGATION OF AURORAL HISS TO THE GROUND

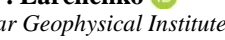
A.S. Nikitenko 📵

Polar Geophysical Institute KSC RAS,

Apatity, Russia, alex.nikitenko91@gmail.com

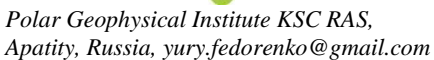
O.M. Lebed 📵

Polar Geophysical Institute KSC RAS, Apatity, Russia, olga.m.lebed@gmail.com A.V. Larchenko



Polar Geophysical Institute KSC RAS, Apatity, Russia, alexey.larchenko@gmail.com

Yu.V. Fedorenko 📵



Abstract. We analyze the effect of changes in the cosmic radio noise absorption in the lower ionosphere on propagation of the auroral hiss to the ground, using observational data from the Lovozero and Tumanny observatories. Three bursts of auroral hiss have been examined whose termination is accompanied by an increase in riometric absorption up to 0.6-2.2 dB. Modeling their propagation from the magnetosphere to the ground under conditions of a perturbed electron density profile, caused by precipitation of energetic electrons, shows that even a small absorption of 0.6 dB in the ionosphere causes the auroral hiss to weaken by 45-50 dB relative to its power at an altitude of 800 km. Calculations show that with such absorption the auroral hiss power near the ground is comparable to the level of natural noise of the Earth — ionosphere waveguide, and with riometric absorption of 2.2 dB a complete termination of the auroral hiss on the ground can be expected.

Keywords: auroral hiss, ionosphere, cosmic noise absorption.

INTRODUCTION

At high latitudes, auroral hiss is one of the most frequently recorded types of natural emissions of magnetospheric origin [Sazhin et al., 1993; Sonwalkar, Harikumar, 2000; Makita, 1979]. In the Russian literature, such emissions are often referred to as auroral hiss — noise emission detected in a wide frequency range 0.3-10 kHz and larger, which includes the VLF band (very lowfrequency, 3-30 kHz). The power spectrum of the hiss magnetic field near the ground is maximum at frequencies 8-10 kHz [Sazhin et al., 1993]; the upper limit may be as great as 30 kHz [Sazhin et al., 1993; Makita, 1979]. Generation of auroral hiss is thought to be associated with precipitation of soft electrons with energies 0.1-10 keV [Sonwalkar, Harikumar, 2000; Makita, 1979].

In the equatorial region of the auroral oval, auroral hiss is most often recorded between 20 and 01 MLT under weak geomagnetic activity ($K_p < 3$) [Kleimenova et al., 2019]. Bursts of these emissions are typical of the magnetospheric substorm growth phase. With the onset of a substorm during auroral breakup, auroral hiss may suddenly disappear [Manninen et al., 2020].

It is believed that the reason for the sudden disappearance of hiss during a breakup may be VLF wave absorption caused by an increase in energetic electron precipitation at this time. Early works dealing with auroral hiss have observed that it is related to riometric absorption variations. Thus, Harang and Larsen [1965] noted that the level of ionospheric absorption affects the ability of auroral hiss to penetrate to the ground. At moderately weak absorption levels, hiss positively correlates with a change in absorption, but at high absorption levels it disappears [Jørgensen, 1966].

We can assume that its disappearance during an auroral breakup occurs for two reasons: 1) hiss generation ceased; 2) due to increased absorption in the lower ionosphere, hiss weakened to the level of natural noise of the Earth-ionosphere waveguide. In this paper, using a complete solution of the wave equation in a plane-stratified medium, we examine the effect of observed riometric absorption bursts on auroral hiss attenuation.

EXPERIMENT 1.

The paper is based on observations of auroral hiss and riometric absorption on the Kola Peninsula at the Lovozero Observatory (67.97° N, 35.02° E) and at the Tumanny Observatory, which is located 100 km north of Lovozero (69.07° N, 35.73° E). We have analyzed events in which recording of auroral hiss stopped after a burst of riometric absorption. VLF fields were measured at the Lovozero Observatory with a three-component receiver [Pil'gaev et al., 2021]. Riometric absorption was measured using riometers at the Lovozero and Tumanny observatories. These riometers operate at a frequency of 38.5 MHz, and their receiving antennas have an angular aperture of 44°.

We used recordings made between September 1 and December 31, 2023. We have examined three characteristic events when hiss bursts were recorded at the Lovozero Observatory, after which cosmic radio noise absorption increased up to 0.6-2.2 dB at both observatories. They took place on November 9

at 20:00–21:00 UT (event 1), on December 7 at 21:00–22:00 UT (event 2), and on December 15 at 19:00–20:00 UT (event 3).

Figure 1 presents magnetograms from the International Monitor for Auroral Geomagnetic Effects (IM-[https://space.fmi.fi/image/www/index.php], spectrograms of the magnetic field horizontal component in the frequency range 1-11 kHz from the Lovozero Observatory, and plots of the time dependence of the riometric absorption level from the Lovozero and Tumanny observatories for the selected events. The spectrograms were obtained after pre-processing of VLF measurement data, which involved, first of all, suppressing intense impulsive atmospheric noise from lightning discharges (atmospherics). Figure 1 shows that all the three events occurred during the substorm growth phase. It is worth noting that, according to all-sky camera observations at the Lovozero Observatory, at the moment of disappearance of hiss and the simultaneous onset of an increase in riometric absorption, an auroral breakup was recorded (data not shown). Unfortunately, small clouds on December 7 and 15 made it difficult to create keograms of these events.

In events 1 and 2 (panels *a*, *b*), riometric absorption begins to gradually increase to 2.2 and 0.6 dB respectively after disappearance of hiss simultaneously at the spaced observatories. Note that the riometric absorption values close in time and magnitude from the Lovozero and Tumanny observatories suggest that the region of increased riometric absorption in these cases was not local, but occupied a large area. In turn, in event 3 (panel *c*), riometric absorption maxima are shifted (it occurs later at the Tumanny Observatory), which may indicate

that at the time considered (19:29 UT) the disturbance region is local in the vicinity of the Lovozero Observatory. Here, the disappearance of hiss coincides with the moment when the riometric absorption level increases to 0.7 dB.

It is worth noting that in the events of interest hiss disappears when riometric absorption is both 0.6 and 2.2 dB. To find out whether the observed absorption level could lead to a weakening of hiss to the level of natural noise of the Earth—ionosphere waveguide, we have modeled auroral hiss propagation to the ground.

2. MODELING

The riometric absorption increase observed in the experiment is probably related to auroral electron precipitation that often occurs during a magnetospheric substorm. Energies of precipitating electrons can vary from ~100 eV to several hundred kiloelectronvolts, which allows them to penetrate up to the D layer of the ionosphere (60-90 km). To study the riometric absorption effect on the arrival of auroral hiss at the ground, two problems need to be solved: 1) to find electron density profiles $N_{\rm e}$ providing the observed level of riometric absorption; 2) to estimate auroral hiss attenuation during propagation to the ground through the ionosphere for the selected profiles. Such an estimate should include a change in the energy of a downward wave both due to reflection in the region of a large refractive index gradient in the precipitation-modified E layer, and due to its absorption in the lower ionosphere, where a high frequency of electron-neutral particle collisions is observed.

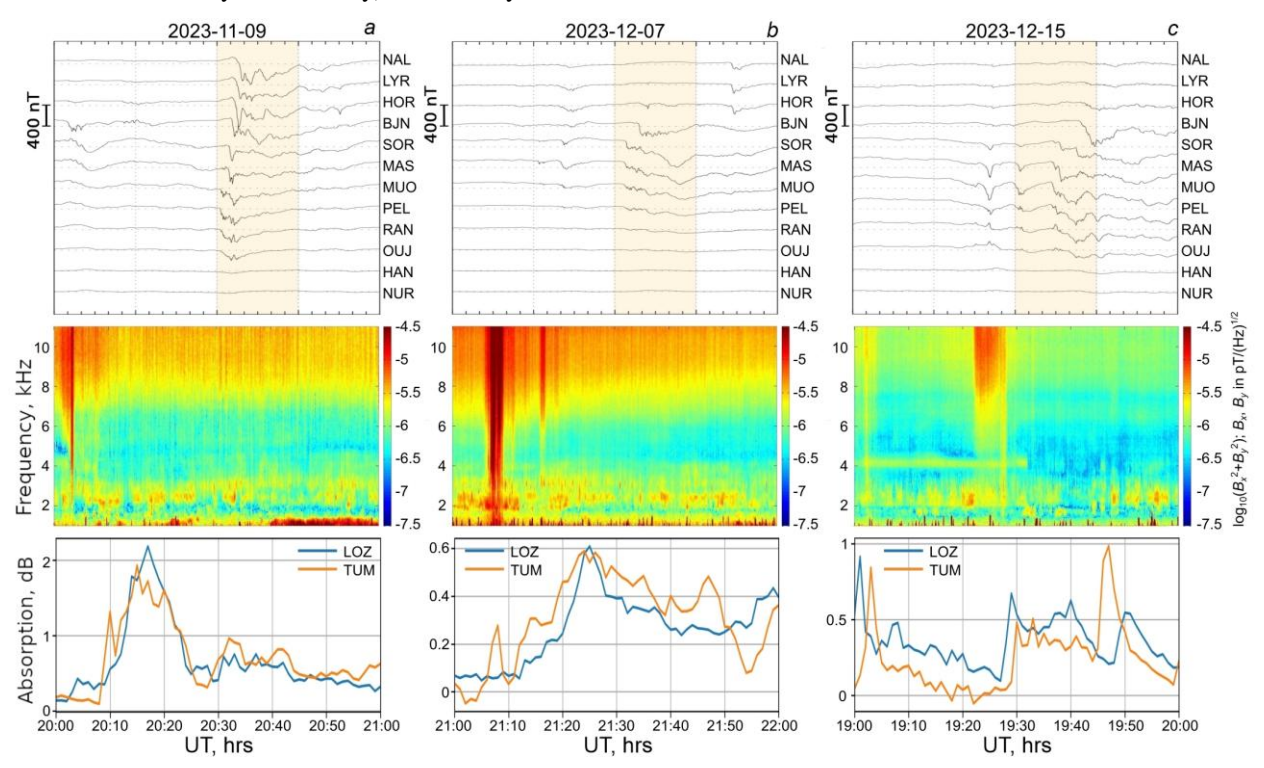


Figure 1. IMAGE magnetograms (top), spectrograms of the magnetic field horizontal component in the frequency range 1–11 kHz from the Lovozero Observatory, and plots of the time dependence of the riometric absorption level from the Lovozero and Tumanny observatories for the events on November 9 at 20:00–21:00 UT (a), December 7 at 21:00–22:00 UT (b), December 15 at 19:00–20:00 UT (c)

To find the necessary $N_{\rm e}$ profiles, we have employed the ionospheric ionization model [Lehtinen, Inan, 2007] that allows us to relate the magnitude of the precipitating electron flux and its energy to changes in the ionospheric profile. To calculate auroral hiss propagation through the modified ionosphere to the ground, we have used the so-called full-wave method based on solving the wave equation in a plane-stratified medium [Lehtinen, Inan, 2008].

Formation of electron density profiles of the disturbed ionosphere

To form $N_{\rm e}$ profiles during high-energy electron precipitation, we made use of the program pyGPI5 [Kaeppler et al., 2022] — implementation of the ionization model in Python [Lehtinen, Inan, 2007]. It is a modification of the so-called Glukhov—Pasko—Inan (GPI) model [Glukhov et al., 1992] designed to calculate the electron density in the E and D layers. In this lower-ionosphere ionization model, five first-order ordinary differential equations are simultaneously solved which describe the time evolution of five groups of particles: electrons, light and heavy positive ions, light and heavy negative ions. From this solution, the $N_{\rm e}$ profile is formed as a response to a given flux of precipitating electrons with specified energies.

To calculate the background density that is used to form additional density driven by energetic electron precipitation, we employed the standard empirical model IRI-2020 [Bilitza et al., 2017]. The neutral particle density and temperature required for calculating the disturbed N_e profile were estimated by the NRLMSISE-00 model [Picone et al., 2002].

The electron transfer model included in the ionization model can define the energy distribution of precipitating electrons by the Maxwellian distribution [Fang et al., 2008] or by a distribution in the form of a set of monoenergetic electron fluxes with discrete energies, taken, for example, from satellite data [Fang et al., 2010]. In this paper, we use the Maxwellian distribution of electrons because, as shown in a number of works, it well describes the distribution of electrons with energies from 100 eV to 1 MeV [Ivanov, Dashkevich, 2019; Troshichev et al., 1986; Frahm et al., 1997]. The differential electron flux used in this model is determined from the expression

$$\phi(E) = \frac{Q_0}{2E_0^3} E \exp\left(-\frac{E}{E_0}\right),$$

where Q_0 [keV·cm⁻²·s⁻¹] is the total energy flux of precipitating electrons; E_0 [keV] is the characteristic energy at which the spectral flux is maximum [Fang et al., 2008]. Next, for convenience, we measured the energy flux of precipitating electrons in mW·m⁻² Q_0 [MW·m⁻²]= Q_0 [keV·cm⁻²·s⁻¹]1.6·10⁻⁹.

We searched for the $N_{\rm e}$ profiles capable of providing experimentally observed values of riometric absorption, using the iterative method by varying the precipitating electron flux energy E_0 and density Q_0 . So, E_0 was varied

from 5 to 100 keV; Q_0 , from 0.2 to 10 MW·m⁻². In this paper, riometric absorption is height-integrated absorption of cosmic radio noise at a frequency of 38.5 MHz.

This frequency is within the frequency range 30–50 MHz optimal for estimating the absorption. Cosmic radio noise measurements at frequencies below 30 MHz require a large antenna, which causes noise to increase. At frequencies above 50 MHz, the sensitivity of the device decreases significantly [Hargreaves, 1969].

To estimate cosmic radio noise absorption [dB] at 38.5 MHz, we employed the expression [Hargreaves, 1969]

$$A = 4.6 \cdot 10^{-5} \int_0^{h_{\text{max}}} \frac{N_e \, \text{v}}{\omega^2 + \text{v}^2} \, dh,$$

where $N_{\rm e}$ is the electron density in m⁻³; v is the frequency of electron-neutral collisions; $\omega = 2\pi f$ is the angular frequency. The integration is carried out over the entire set of layers, into which the ionosphere is divided, from Earth's surface to (in our case) the height $h_{\rm max}$ where whistler waves are scattered.

Note that the main contribution to the total absorption at 38.5 MHz is made by electron-neutral particle collisions at heights below 120 km (D, E layers) [Hargreaves, 1969]. For these heights, the first term prevails in the denominator in the expression for estimating cosmic radio noise absorption A at 38.5 MHz. In this case, the total absorption is proportional to the integral of $N_{\rm e}v$ [Hargreaves, 1969]. The maximum collision frequency is below 120 km, so it is at these heights that the maximum absorption of cosmic radio noise at 38.5 MHz will occur.

The frequency of electron-neutral particle collisions was calculated in accordance with [Banks, 1966].

The model of auroral hiss propagation to the ground

Auroral hiss generation is associated with the development of Cherenkov's instability of precipitating electrons with energies 0.1–10 keV in the magnetosphere at heights ~6-20 thousand km [Sonwalkar, Harikumar, 2000; Makita, 1979]. Auroral hiss that occurs at these heights is a quasi-electrostatic whistler wave with ~90° angle of the wave normal **n** to the magnetic field line. The most complete model of auroral hiss propagation to the ground has been proposed in [Sonwalkar, Harikumar, 2000]. To explain the auroral hiss propagation to the ground, it assumes that quasi-electrostatic waves below 5000 km are scattered by small-scale (<100 m) irregularities in the electron density of ionospheric plasma $n_{\perp} < 1$. As a result, some of the scattered waves have values of the wave normal components horizontal relative to the normal to the ground n_p <1. According to Snell's law, at such values of n_p the waves can reach the ground [Stix, 1992].

Auroral hiss propagation was modeled using the numerical model detailed in [Lebed' et al., 2019]. This model relates all stages of hiss propagation from the generation site to the ground and takes into account the random nature of wave fields. The random field of quasi-

electrostatic waves was formed in a Cartesian coordinate system in which the Z-axis extends in the external magnetic field vector. The generation height was set to 2000 km. The electrons responsible for the generation met two conditions. First, Cherenkov's resonance condition held — overlapping of the projections of the phase velocity of emerging whistler wave $v_{ph} = c / n_z$ and the electron velocity v_{\parallel} on the direction of the external magnetic field line. Here, $\mathbf{n} = [\mathbf{n}_{\perp}, \mathbf{n}_{\perp}]$ is the refractive index vector; $n = \mathbf{k}/\mathbf{k}_0$, where \mathbf{k} is the wave vector. Second, only those electrons for the velocity distribution of which $F(v_{\parallel}) \partial F(v_{\parallel})/\partial v_{\parallel} > 0$ was met were responsible for the generation [Sazhin et al., 1993]. In this work, we use a typical electron energy distribution obtained during rocket measurements in a stable auroral arc [Pulliam et al., 1981]. This distribution has the form of a Maxwellian distribution with a characteristic energy $E_0=3$ keV at which the spectral flux is maximum. When modeling a random field, we assumed that the transverse components n_{\parallel} are evenly distributed over the azimuth angles $p(\varphi) = 1/(2\pi)$, where φ is the azimuth angle of wave normal [Lebed' et al., 2019].

Since high-energy electron precipitation modifies the $N_{\rm e}$ profile mainly at heights <400 km, and at heights >1000 km whistler wave damping is negligible, to solve the problem of estimating the auroral hiss attenuation it will suffice to calculate propagation of auroral hiss, when scattered by small-scale irregularities of the lower ionosphere, to the ground. In this work, the $N_{\rm e}$ irregularities small-scale compared to the wavelength were placed at h_{max} =800 km [Shklyar, Nagano 1998; Nikitenko et al., 2023]. The region with irregularities was assumed to be spatially limited by a two-dimensional Gaussian with standard deviations σ $_x=\sigma$ $_y=50$ km. The result of scattering of quasielectrostatic waves by the layer with irregularities, except for the initial electrostatic wave that does not reach the ground and is further ignored in the model, is a superposition of plane whistler waves with random amplitudes, phases, and directions of wave normals, including in the range $n_{\perp} < 1$.

In calculating propagation of generated quasielectrostatic waves up to the scattering height and scattered waves to the ground, we began to use the Cartesian coordinate system in which the Z-axis is normal to the ground, defined by an infinitely conducting plane. The ionosphere is defined as a plane-stratified medium. This approximation is actively engaged in studying the propagation of VLF waves through the ionosphere [Aksenov, 1975; Lehtinen, Inan, 2008]. Thickness of the layers varied according to the rate of change in $N_{\rm e}$. Strength and direction of the geomagnetic field were calculated by the Tsyganenko model [Tsyganenko, 1995]. To neglect the influence of waves reflected from the ground on the calculation results, we set conditions for free departure of waves at the lower boundary of a medium coinciding with the ground [Lebed' et al., 2019].

By calculating scattered wave field components, we can estimate the auroral hiss integral power in each layer. To do this, we integrated the modulus of the Poynting vector's vertical component over the area. The ratio of the hiss integral power in a particular layer to the power in the upper layer [dB] characterizes whistler wave damping during propagation. Denote it by $A_{\rm hiss}$.

3. MODELING RESULTS

In event 1 (see Figure 1), riometric absorption runs to 2.2 dB. Figure 2, a shows several possible $N_{\rm e}$ profiles providing 2.2±0.1 dB absorption and calculated by the pyGPI5 program. The $N_{\rm e}$ profile calculated by IRI-2020 for November 9, 2023 at 20:00 UT was taken as the background. The calculation has revealed that, as in the experiment, cosmic radio noise absorption can occur at characteristic energies of precipitating electrons $E_0>10$ keV. We can see that the higher the energy of precipitating electrons, the lower they penetrate into the ionosphere. Thus, the presence of 50 keV electrons leads to maximum $N_{\rm e}$ at a height of 79 km.

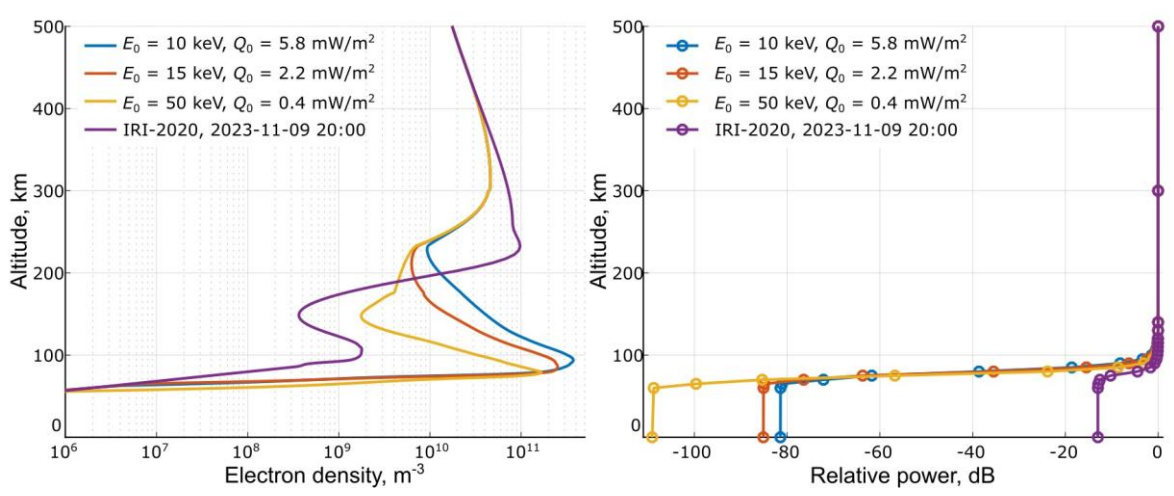


Figure 2. Event modeling — ionospheric N_e profiles (a): background, obtained by IRI-2020, and disturbed, which can provide 2.2 ± 0.1 dB riometric absorption; b — height dependences of whistler wave relative power $A_{hiss}(h)$ corresponding to these profiles

Panel b presents the calculated height dependences of the whistler wave relative power $A_{hiss}(h)$ corresponding to the profiles shown in panel a. A_{hiss} is seen to begin decreasing sharply from a height of ~100 km, where there is increased N_e . For the quiet background N_e profile, the total damping of the whistler wave after passing from the scattering region to the ground through the ionosphere was ~13 dB. According to our long-term observations, the ratio of the average hiss power near the ground to the noise power of the Earth—ionosphere waveguide ranges from 30 to 40 dB. It is caused by attenuation of hiss when passing through the ionosphere and propagating in the Earth—ionosphere waveguide to the detection station. Hence, according to the modeling results, the hiss signal-to-noise ratio over the ionosphere should be by 10-20 dB higher, i.e. ~40-50 dB. Figure 2 indicates that the $N_{\rm e}$ profiles perturbed by precipitating electrons cause auroral hiss of 80 dB and higher to attenuate. In this case, the signal-to-noise ratio on the ground will be lower than -40 dB, which is approximately 10⁻⁴ of the auroral hiss signal power over the ionosphere. Obviously, with these perturbed $N_{\rm e}$ profiles it is simply impossible to observe auroral hiss on the ground.

Events 2 and 3 were modeled in a similar way. Riometric absorption on December 7 and 15, 2023 was 0.6 and 0.7 dB respectively (see Figure 1). Since the riometric absorption values are so close, we examine these events together.

Figure 3 presenting the modeling results for events 2 and 3 is similar to Figure 2. The background profiles obtained by IRI-2020 are seen to almost coincide because of close dates and times (December 7, 21:00 UT and December 15, 19:00 UT). In these cases, among the $N_{\rm e}$ profiles leading to experimental riometric absorption values were those formed by distributions of precipitating electrons with characteristic energies E_0 =5 keV, i.e. electrons from the same energy range as those responsible for the generation of auroral hiss [Sonwalkar, Harikumar, 2000]. Since the penetration depth of 5–15 keV electrons into the ionosphere is smaller, $N_{\rm e}$ maxima

(compared to event 1) are slightly higher here, at ~90 km. In this case, precipitating electrons are seen to cause whistler waves to weaken by ~45–50 dB. Here, the signal-to-noise ratio on the ground will be ~–5 dB, which is 0.3 of the auroral hiss signal power over the ionosphere. Since in this case the auroral hiss signal power is comparable to or less than the natural noise level of the Earth—ionosphere waveguide, auroral hiss will not be detected in the electromagnetic field data either. Thus, the experimentally observed disappearance of hiss at the Lovozero Observatory, accompanied by a simultaneous increase in riometric absorption during the onset of a substorm, is most likely caused by deterioration in the conditions of whistler wave propagation in the lower ionosphere.

DISCUSSION AND CONCLUSIONS

In event 3, hiss bursts end simultaneously with a sharp increase in riometric absorption up to 0.5–0.6 dB. According to the modeling results, with such absorption the ionosphere becomes opaque to hiss, which leads to an abrupt cessation of its recording near the ground. In events 1 and 2, hiss bursts terminate a few minutes before maximum absorption at the Lovozero and Tumanny observatories.

Events 1 and 2 are first characterized by the occurrence of a powerful hiss burst, followed by a series of weaker bursts. In both events, the hiss power decreases simultaneously with increasing riometric absorption. In event 1, the burst power decreases after an increase in the absorption level to 0.3 dB at the Lovozero Observatory. In event 2, the power of bursts gradually decreases at the same time as riometric absorption gradually increases. Hiss disappears when riometric absorption runs to ~0.5 dB, i.e. when, according to the modeling results, the ionosphere becomes opaque to hiss. In event 1, hiss disappears at 20:10 UT, 7–8 min before maximum absorption; and in event 2, at 21:20 UT, ~1 min before the maximum.

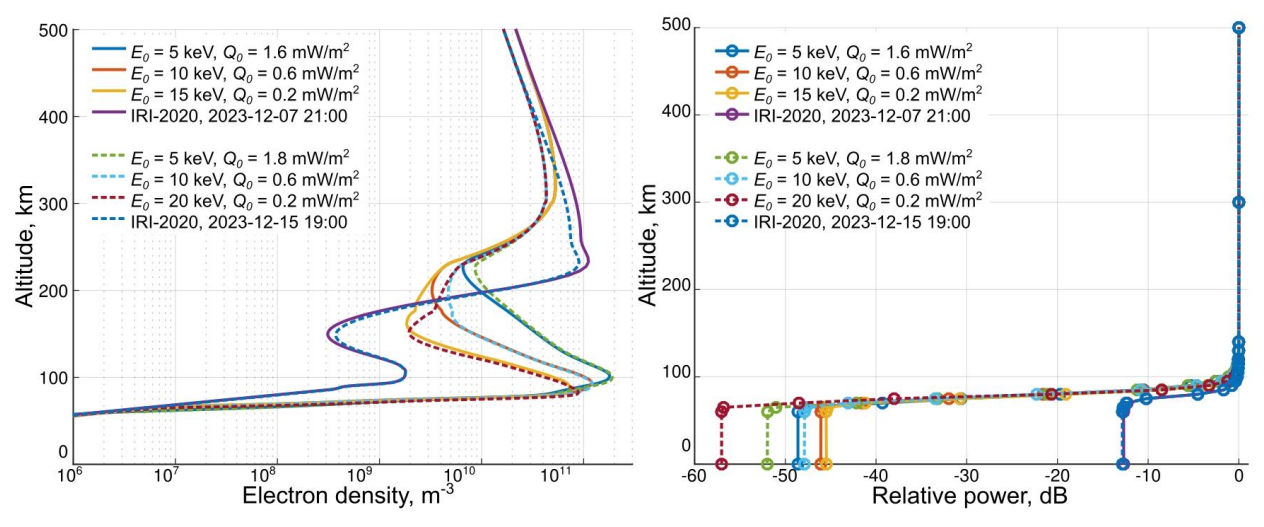


Figure 3. Modeling of events 2 and 3 — N_e profiles (left): background, obtained by IRI-2020, and perturbed, which can provide riometric absorption 0.6 ± 0.1 dB (solid lines) and 0.7 ± 0.1 dB (dashed lines). To the right are height dependences of whistler wave relative power $A_{hiss}(h)$ corresponding to these profiles

To explain the effect of auroral hiss disappearance with an increase in riometric absorption to 0.6-2.2 dB, we modeled auroral hiss propagation to the ground under conditions of unperturbed $N_{\rm e}$ profile and that perturbed by precipitation of energetic electrons with Maxwellian velocity distribution and different flux densities Q_0 and characteristic energy E_0 . It has been found that an increase in riometric absorption even up to 0.6 dB causes hiss to weaken by 45-50 dB relative to its power at 800 km. In this case, the hiss power near the ground becomes comparable to the intrinsic noise power of the Earth—ionosphere waveguide. At a riometric absorption level of 2.2 dB, we can expect complete cessation of hiss recording on the ground.

This work was financially supported by RSF grant No. 24-27-20048 "Estimate of ionospheric conditions in the Arctic zone from results of ground-based measurements of both the electromagnetic field of auroral hisses in a very low frequency range and riometric absorption"

REFERENCES

- Aksenov V.I. Investigation of the propagation of very long radio waves in the Earth's ionosphere. 1. Theory. *Radiophysics and Quantum Electronics*. 1975, vol. 18, pp. 985–995.
- Banks P. Collision frequencies and energy transfer electrons. *Planet. Space Sci.* 1966, vol. 14, no. 11, pp. 1085–1103.
- Bilitza D., Altadill D., Truhlik V., Shubin V., Galkin I., Reinisch B., Huang X. International reference ionosphere 2016: From ionospheric climate to real-time weather predictions. *Space Weather*. 2017, vol. 15, no. 2, pp. 418–429. DOI: 10.1002/2016SW001593
- Fang X., Randall C.E., Lummerzheim D., Solomon S.C., Mills M.J., Marsh D.R., Jackman C.H., Wang W., Lu G. Electron impact ionization: A new parameterization for 100 eV to 1 MeV electrons. *J. Geophys. Res.* 2008, vol. 113, A09311. DOI: 10.1029/2008JA013384.
- Fang X., Randall C.E., Lummerzheim D., Wang W., Lu G., Solomon S.C., Frahm R.A. Parameterization of monoenergetic electron impact ionization. *Geophys. Res. Lett.* 2010, vol. 37, L22106. DOI: 10.1029/2010gl045406.
- Frahm R.A., Winningham J.D., Sharber J.R., Link R., Crowley G., Gains E.E., Chenette D.L., Anderson B.J., Potemra T.A. The diffuse aurora: A significant source of ionization in the middle atmosphere. *J. Geophys. Res.* 1997, vol. 102, no. D23, pp. 28,203–28,214. DOI: 10.1029/97JD02430.
- Glukhov V.S., Pasko V., Inan U.S. Relaxation of transient lower ionospheric disturbances caused by lightning-whistler-induced electron precipitation bursts. *J. Geophys. Res.* 1992, vol. 97, pp. 16971–16979. DOI: 10.1029/92JA01596.
- Harang L., Larsen R. Radio wave emissions in the VLF-band observed near the auroral zone I. Occurrence of emissions during disturbances. *J. Atmos. Terr. Phys.* 1965, vol. 27, pp. 481–497. DOI: 10.1016/0021-9169(65)90013-9.
- Hargreaves J.K. Auroral absorption of HF radio waves in the ionosphere: A review of results from the first decade of riometry. *Proc. IEEE*. 1969, vol. 57, pp. 1348–1373. DOI: 10.1109/PROC.1969.7275.
- Ivanov V.E., Dashkevich Zh.V. About the possibility of researching of the spectra of precipitating electrons by using optical observations of MAIN system. *Transactions Kola Science Centre*. 2019, vol. 8, no. 5. DOI: 10.25702/KSC.2307-5252.2019.10.8.
- Jørgensen T.S. Morphology of VLF hiss zones and their corre-

- lation with particle precipitation events. *J. Geophys. Res.* 1966, vol. 71, no. 5, pp. 1367–1375. DOI: 10.1029/JZ071i 005p01367.
- Kaeppler S.R., Marshall R., Sanchez E.R., Juarez Madera D.H., Troyer R., Jaynes A.N. PyGPI5: A python D- and E-region chemistry and ionization model. *Front. Astron. Space Sci.* 2022, vol. 9, pp. 1–10. DOI: 10.3389/fspas.2022.1028042.
- Kleimenova N., Manninen J., Gromova L., Gromov S., Turunen T. Bursts of auroral-hiss VLF emissions on the Earth's surface at 1~5.5 and geomagnetic disturbances. *Geomagnetism and Aeronomy*. 2019, vol. 59, no 3, pp. 272–280. DOI: 10.1134/S0016793219030083.
- Lebed', O.M., Fedorenko, Y.V., Manninen, J., Kleimenova N.G., Nikitenko A.S. Modeling of the auroral hiss propagation from the source region to the ground. *Geomag*netism and Aeronomy. 2019, vol. 59, pp. 577–586. DOI: 10.1134/S0016793219050074.
- Lehtinen N.G., Inan U.S. Possible persistent ionization caused by giant blue jets. *Geophys. Res. Lett.* 2007, vol. 34, L08804. DOI: 10.1029/2006GL029051.
- Lehtinen N.G., Inan U.S. Radiation of ELF/VLF waves by harmonically varying currents into a stratified ionosphere with application to radiation by a modulated electrojet. *J. Geophys. Res.* 2008, vol. 113, A06301. DOI: 10.1029/2007JA012911.
- Makita K. VLF/LF hiss emissions associated with aurora. *Mem. Natl. Inst. Polar Res. Tokyo. Ser. A.* 1979, No. 16, pp. 1–126.
- Manninen J., Kleimenova N., Kozlovsky A., Fedorenko Y., Gromova L., Turunen T. Ground-based auroral hiss recorded in Northern Finland with reference to magnetic substorms. *Geophys. Res. Lett.* 2020, vol. 47, e2019GL086285. DOI: 10.1029/2019 GL086285.
- Nikitenko A.S., Fedorenko Yu V., Manninen J., et al. Modeling the spatial structure of the auroral hiss and comparing results to observations. *Bull. Russian Academy of Sciences: Physics.* 2023, vol. 87, no. 1, pp. 112–117. DOI: 10.3103/s1062873822700265.
- Picone J.M., Hedin A.E., Drob D.P., Aikin A.C. NRLMSISE-00 empirical model of the atmosphere: Statistical comparisons and scientific issues. *J. Geophys. Res.* 2002, vol. 107, iss. A12, CiteID 1468. DOI: 10.1029/2002JA009430.
- Pil'gaev, S.V., Larchenko, A.V., Fedorenko, Yu.V., Filatov M.V., Nikitenko A.S. A three-component very-lowfrequency signal receiver with precision data synchronization with universal time. *Instruments and Experimental Techniques*. 2021, vol. 64, pp. 744–753. DOI: 10.1134/S0020 441221040229.
- Pulliam D.M., Anderson H.R., Stamnes K., Rees M.H. Auroral electron acceleration and atmospheric interactions: (1) Rocket-borne observations and (2) Scattering calculations. J. Geophys. Res.: Space Phys. 1981, vol. 86, no. A4, pp. 2397–2404. DOI: 10.1029/JA086iA04p02397.
- Sazhin S.S., Bullough K., Hayakawa M. Auroral hiss: a review. *Planet. Space Sci.* 1993, vol. 41, pp. 153–166. DOI: 10.1016/0032-0633(93)90045-4.
- Shklyar D.R., Nagano I. On VLF wave scattering in plasma with density irregularities. *J. Geophys. Res.: Space Phys.* 1998, vol. 103, no. A12, pp. 29515–29526. DOI: 10.1029/98JA02311.
- Sonwalkar V.S., Harikumar J. An explanation of ground observations of auroral hiss: Role of density depletions and meter-scale irregularities. *J. Geophys. Res.: Space Phys.* 2000, vol. 105, no. A8, pp. 18867–18883. DOI: 10.1029/1999JA000302.

Stix T. Waves in Plasmas. American Inst. Phys. 1992.

Troshichev O.A., Besprozvannaya A.S., Makarova L.N. Ionospherno-magnitnie vozmuscheniya v vysokih shirotah. - pod redakciey O.A. Troshicheva. L.: AANII, Gidrometeoizdat, 1986, 255 p. (In Russian).

Tsyganenko N.A. Modeling the Earth's magnetospheric magnetic field confined within a realistic magnetopause. *J. Geophys. Res.* 1995, vol. 100, pp. 5599–5612. DOI: 10.1029/94JA03193.

URL: https://wdc.kugi.kyoto-u.ac.jp/dst_provisional/index.html (accessed November 14, 2024).

Original Russian version: Nikitenko S.A., Lebed O.M., Larchenko A.V., Fedorenko Yu.V., published in Solnechno-zemnaya fizika. 2025, vol. 11, no. 1, pp. 70–76. DOI: 10.12737/szf-111202508. © 2025 INFRA-M Academic Publishing House (Nauchno-Izdatelskii Tsentr INFRA-M)

How to cite this article

Nikitenko S.A., Lebed O.M., Larchenko A.V., Fedorenko Yu.V. Analysis of the effect of cosmic noise absorption increase on propagation of auroral hiss to the ground. *Solar-Terrestrial Physics*. 2025, vol. 11, iss. 1, pp. 63–69. DOI: 10.12737/stp-111202508.